Orientational effects in the channel flow of flexible and rigid molecules

Y. Radzyner and D. C. Rapaport
Department of Physics, Bar-Ilan University, Ramat-Gan 52900, Israel
(Received 26 November 1997)

Short linear molecules exhibit rotational motion and orientational preferences under sheared flow. This paper describes a series of molecular-dynamics simulations of fluids consisting of various kinds of short linear chain molecules that are forced to flow through a channel bounded by rough, parallel walls (Poiseuille flow). The molecules are constructed of soft spheres; these are linked in different ways to produce either fully flexible chains, stiff chains with restricted internal degrees of freedom, or rigid rodlike molecules. The channel walls act as nonslip boundaries and also serve to absorb the thermal energy generated by the shear motion. For each kind of molecule, the rotational motion and orientation distributions are explored as functions of the cross-stream position. The variation in orientation shows that there is a competition between the Maxwell orientation, where the molecule is aligned at 45° to the flow, and a tendency for molecules close to the walls to align parallel to the direction of flow. The orientational effects become more pronounced with increasing molecular stiffness. [S1063-651X(98)00305-5]

PACS number(s): 47.50.+d, 02.70.Ns, 36.20.Ey, 47.60.+i

I. INTRODUCTION

The fact that continuum hydrodynamic theory does not deal with fluids at the discrete atomistic level complicates the inclusion of effects due to molecular conformation, entanglement, orientation, and rotation into the fluid dynamical equations. The exotic rheological properties exhibited by polymer liquids [1] are an example of the kind of behavior not readily addressed within a conventional continuum framework. As the length and time scales that can be covered using discrete-particle molecular-dynamics (MD) simulation increase there is hope that MD will eventually be able to probe some of the microscopic aspects of these phenomena, at least those that occur on sufficiently short time scales. The difficulty with MD simulation is that its rate of progress is governed by the fastest dynamical processes occurring in the system and the numerical integration of the equations of motion is forced to use a sufficiently small time step to faithfully represent the rapid internal motions of the molecules; the large-scale rearrangements that are of rheological relevance occur over time intervals that are typically orders of magnitude larger and it is this disparity that has so far proved insurmountable. However, the alternative seems even less promising: given the complexity of the behavior it appears unlikely that a continuum approach (based on some appropriate extension of the Navier-Stokes formulation), which even fails to acknowledge the underlying molecular nature of the fluid, is capable of offering a quantitative explanation for the underlying mechanisms.

In this paper we address a more limited problem, namely, the nature of the molecular behavior in a fluid of short linear molecules (oligomers) undergoing sheared flow. We consider three different types of molecule, ranging in nature from the completely flexible, subject only to excluded volume effects, to the completely rigid, and examine the rotational motion and orientational effects that appear as a consequence of the sheared motion. Short molecules clearly lack important effects such as chain entanglement, so that while related to the more complex long-term goal enunciated above, the present work does not demand the enormous computational resources that would otherwise be required, but at the same time produces results that are relevant to the subject and interesting in their own right. An earlier study [2] dealt with a portion of this problem; it was, however, based on an alternative form of MD methodology involving hard spheres, rather than the soft spheres of the present work, and the technique does not lend itself to dealing with more complex models, including the rigid case described here.

Channel or Poiseuille flow is one of the few situations in fluid dynamics for which, under suitable assumptions, a full analytic solution is available: It is indeed a classic textbook exercise [3]. The form of the hydrodynamic equations used to describe the problem assumes a Newtonian (constant viscosity) fluid at constant density. Such a problem might seem remote from the system studied here, but it turns out that despite the far more complex behavior of the chain molecules (that is indicative of a position-dependent viscosity whose value depends on the strongly varying local flow conditions), the analytic solution remains applicable.

The effect of shear on molecular orientation in fluids has a lengthy history, extending back at least as far as Maxwell's description of the optical birefringence that occurs in flowing Canada balsam [4]. There have been a number of MD studies of uniformly sheared (Couette) flow of short model alkane chains [5–7]. It has also proved possible to eliminate any extraneous influence of the channel walls by the use of sliding periodic boundaries [7] (in some cases also imposing a constant sprain rate); given the very small systems studied in some of the earlier work, the ability to eliminate walls and so achieve a homogeneous Couette system free of wall surface artifacts (although still subject to finite-size effects in other respects) proved particularly advantageous. In the case of dimer fluids, both Couette [8] and Poiseuille [9] flows have been simulated. Sheared polymer flows, both uniform and oscillatory, are potentially important as industrial methods for creating aligned polymeric nanostructures [10]; the absence of a theoretical description of the behavior at the atomistic level is a strong motivating factor for treating prob-

lems of this kind by means of numerical simulation.

II. COMPUTATIONAL METHODOLOGY

The simulations involve highly simplified models that attempt to represent the principal features of short linear molecules. The most important of these properties is the excluded volume effect; each molecule is constructed from a permanently linked sequence of spherical monomers and overlap between these monomers, irrespective of whether they belong to the same molecule or different molecules, is prevented by means of a strong but short-ranged repulsive interaction (the details appear later). Maintaining the connectivity in flexible chains is achieved by introducing narrow potential wells between pairs of bonded neighbors [11,12]; the parameters of this interaction are adjusted to limit the allowed variation in monomer separation to a small fraction of the nominal bond length. The maximum separation of bonded monomers is chosen to be sufficiently small so that chains are unable to penetrate one another.

The chain model just described is completely flexible, subject only to the limitations imposed by the excluded volume. This represents the first kind of model studied in the present work. In the second model a certain amount of stiffness is introduced by limiting the range of variation of the angles between adjacent bonds (two bonds sharing a common monomer); to achieve this goal a steep potential well between next-nearest-neighbor monomers is imposed to limit the minimum and maximum separations, thereby confining the bond angle to a narrow range around the desired value. There is a limit to the degree of rigidity that can be produced by this mechanism since the frequency of the oscillation associated with the additional potential well increases as the well is made narrower and so the completely rigid chain, the third kind of system studied here, is modeled in a different manner. A massless linear rigid body is introduced and the monomers are positioned at fixed, equally spaced sites along its axis (the spacing is equal to the mean bond length of the flexible chains); each monomer contributes its own mass to the molecule and acts as an interaction site for determining the forces between molecules.

The overlap repulsion between soft-sphere monomers located at $\boldsymbol{r}_i$ and $\boldsymbol{r}_j$ is described by means of a truncated Lennard-Jones potential

$$V_{ss}(r_{ij})=4\epsilon\left[\left(\frac{\sigma}{r_{ij}}\right)^{12}-\left(\frac{\sigma}{r_{ij}}\right)^{6}+\frac{1}{4}\right], \tag{1}$$

where $\boldsymbol{r}_{ij}=\boldsymbol{r}_i-\boldsymbol{r}_j$, and $r_{ij}=|\boldsymbol{r}_{ij}|$, and with a cutoff imposed at a range $r_{ij}=r_c=2^{1/6}\sigma$; note that the potential tends smoothly to zero at the cutoff, i.e., $V_{ss}(r_c)=dV_{ss}(r_c)/dr=0$. The interaction used to preserve the bonds between nearest neighbors is based on a potential well that is the sum of two functions; close approach is prevented by the usual $V_{ss}(r)$, while bond extension is governed by a potential with the same functional form but acting in the reverse direction with a suitably shifted origin,

$$V_{nn}(r)=V_{ss}(r)+V_{ss}(r_b-r). \tag{2}$$

The length r_b is an adjustable parameter that can be set to limit the maximum bond extension; measurements show that if $r_b=2r_c$, the bond length fluctuations are limited to approximately 10% of the mean for a system in equilibrium. Additional discussion of this model appears elsewhere [13].

A very similar approach is used to restrict the variation in bond angle around a chosen value, thereby producing a chain with reduced flexibility (the so-called stiff chain). The additional potential has the form

$$V_{nnn}(r)=V_{ss}(r-r_a+r_b/2)+V_{ss}(r-r_a-r_b/2) \tag{3}$$

and this is applied to next-nearest-neighbor monomers. For the system considered here, a mean bond angle of 15° is achieved by setting

$$r_a=2\cos(\pi/24)r_c. \tag{4}$$

From the MD point of view, both of these systems are essentially fluids of spherically symmetric particles (the monomers) moving under the forces acting between their centers. After evaluating the forces on the monomers, all that is required for the MD computation is the integration of the translational equations of motion. Rigid molecules, on the other hand, require both translational and rotational motion to be taken into account. The only forces involved in this case are those acting between monomers on different molecules. Once these forces have been determined, the torque acting about the center of mass of each molecule and the total force on the molecule are readily evaluated. The translational equations of motion for the centers of mass are the usual ones, but the rotational equations require special consideration [13] because a linear molecule (in which the monomers themselves have no inherent rotational motion) has only two rotational degrees of freedom, rather than the three normally associated with rigid body motion. If $\boldsymbol{s}_i$ denotes the unit vector along the axis of a molecule, then the rotation equation of motion is

$$\ddot{\boldsymbol{s}}_i=I^{-1}\boldsymbol{\tau}_i\times\boldsymbol{s}_i-\dot{\boldsymbol{s}}_i^2\boldsymbol{s}_i, \tag{5}$$

where $\boldsymbol{\tau}_i$ is the torque and I the moment of inertia. The actual angular velocity is not required for integrating the equations of motion, but when needed its value can be obtained from

$$\boldsymbol{\omega}_i=\boldsymbol{s}_i\times\dot{\boldsymbol{s}}_i. \tag{6}$$

The interaction computations dominate the computational effort. In order to make them more efficient the neighbor list method (details of this and other technical aspects of MD simulation appear in [13]) is used to reduce the number of potentially interacting monomer pairs to a small multiple of the total number of monomers. The neighbor list identifies pairs of monomers that are either within interaction range or just a little outside and it is rebuilt automatically whenever the cumulative monomer motion is sufficient for new interacting pairs to appear that are not present in the list. Integration of the equations of motion for the system of rigid molecules uses a predictor-corrector method with a time step $\Delta t=0.001$, in reduced MD units where $\epsilon=1$, $\sigma=1$, and the monomer mass is unity. In the case of flexible and stiff chains the simpler leapfrog integration method is used and the time step increased to $\Delta t=0.0025$.

The MD approach described here is entirely different from the one used in an earlier series of simulations [2]. The technique used there involved event-driven MD, where the monomers themselves are represented by elastically colliding hard spheres and instead of requiring the solution of the equations of motion over a series of equally-sized time steps, the evolution of the hard-sphere fluid proceeds via a sequence of impulsive collisions. A chain molecule can be constructed in a manner that resembles a ''bead necklace,'' in which spherical monomers are linked by bonds whose length can vary freely, but only over a very limited range. Such bonds are readily incorporated into the event-driven MD framework by introducing collisions of a special type that serve to prevent bond breakage. In order to provide a certain amount of molecular rigidity, bonds of a similar kind are also introduced between next-neighbor monomers in order to limit the range of allowed distances between them as well and thereby, indirectly, the range of allowed bond angles. This kind of approach is less convenient than one based on continuous potentials since the models cannot be extended to include, for example, torsional interactions; there is also the problem that as the range of allowed (nearest or next-nearest) bond variation is reduced, the amount of computation associated with the bond collisions tends to grow rapidly. The approach is also not readily modified to accommodate rigid molecules. Overall, because of its greater capacity for generalization, the soft-sphere approach is the method of choice for problems of this kind.

The opposing effects of an applied driving field and nonslip channel walls produce the sheared flow. A uniform ''gravitational'' acceleration g drives the flow in the y direction; in principle, this is equivalent to a pressure head. The two channel walls parallel to the yz plane are constructed of planar arrays of fixed spherical particles identical to those used for the monomers, which are arranged on a square lattice with a lattice spacing r_c. The interaction of the chain monomers with the wall particles corresponds to an effectively corrugated wall and it is this roughness alone that produces the essentially zero flow rate in a thin fluid layer adjacent to each wall. The other two pairs of region boundaries are periodic.

The sheared motion is a source of viscous heating and this excess heat must be extracted from the system through the walls to avoid a gradual overall temperature rise. The scheme chosen for heat removal depends on whether or not the molecules are rigid. In the case of the flexible and stiff molecules, each individual monomer within interaction range of any of the wall spheres has its velocity rescaled so that the average kinetic energy of all monomers close to the wall equals the specified wall temperature (in this case unity). Rigid molecules are treated somewhat differently. In this case, if any interaction site belonging to a molecule lies within range of a wall particle, both the translational and rotational velocities of the molecule are rescaled to the correct wall temperature; while such a scheme might be questionable for long, rodlike molecules, here the rods are sufficiently short not to cause concern. In both instances the velocity rescaling is only applied if the velocity component normal to the wall (the x direction) is directed towards the channel interior; this is to avoid the risk, however unlikely, of a molecule making use of this mechanism to tunnel through the wall. All schemes of this kind are somewhat arbitrary and reflect the difficulty of incorporating realistic, thermally conducting walls into MD simulations without introducing excessive complexity; one such example involves walls in which the constituent particles are allowed a limited degree of motion [14], but are also coupled to a fictitious heat bath. The measured results indicate that this simplest of wall models performs adequately, in that it not only ensures a practically flow-free zone close to each wall, but also successfully prevents any temperature buildup after the system has reached the steady flow state.

The initial state of the system is tailored to avoid possible overlap of the molecules. The molecular centers of mass are located at the sites of a cubic lattice and the chains are oriented normal to the walls (the z direction) and assigned random velocities. The initial molecular array consists of 45 molecules in both the x and y directions; in the z direction the array is three deep. All chains consist of four monomers (the rigid molecule has four interaction sites) and the initial conformation of the flexible and stiff chains are chosen so that all bonds are at their equilibrium lengths. The overall size of the system is $50.5\times51.5\times13.5$, corresponding to a total monomer density close to 0.7.

The only spatial variation in behavior occurs in the x direction; because of the periodic boundaries in the y and z directions the properties are translationally invariant in any plane parallel to the walls (the yz plane). In order to analyze the behavior of the system, the simulation region is divided into slices parallel to this plane, with each slice covering a narrow range of x values, and the average molecular properties are evaluated for each slice. There is a certain degree of arbitrariness in assigning spatially extended molecules to a particular slice whose thickness is less than the molecular length; the simple scheme used here is to attribute properties associated with the molecule as a whole (e.g., angular momentum and end-to-end distance) to the slice containing the center of mass of the molecule, but for properties more closely associated with individual monomers (e.g., velocity of flexible chains) to assign the measurement to the slice containing the actual monomer. The presence of secondary flows (periodic or other deviations from a flow that otherwise depends only on the x coordinate) would require a more detailed analysis, but this problem does not arise at the flow speeds (and corresponding Reynolds numbers) considered here.

III. RESULTS

Each simulation run begins with no overall flow, but under the influence of the driving force there is a gradual velocity buildup. The heat-absorbing, nonslip boundaries ensure that a time-invariant flow pattern eventually emerges (assuming the driving force is not excessively strong), although the number of integration steps required to reach this state, as well as the maximum flow speed at the stream midpoint, depends on the various parameters of the system, including the channel width. The run is allowed to reach a steady flow state before starting to make flow measurements; typically, for the systems described here, approximately 400 (reduced) time units are required to reach the limiting state. There is a tendency for the flow speed to overshoot its lim-

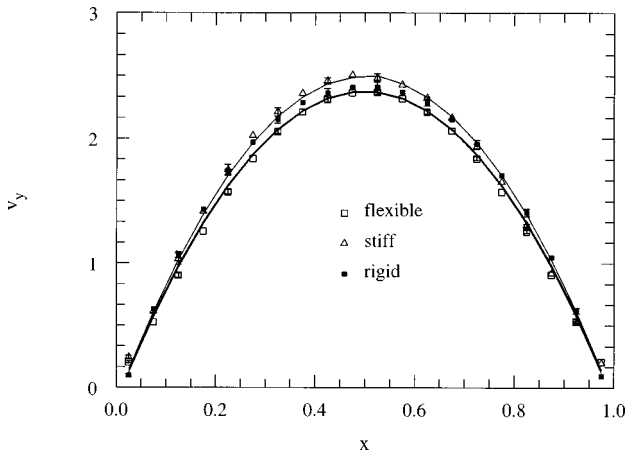

FIG. 1. Cross-stream velocity profiles for the flexible, stiff, and rigid molecules (x is the normalized cross-stream coordinate); the curves show the results of quadratic fits and typical (very small) error bars are also shown.

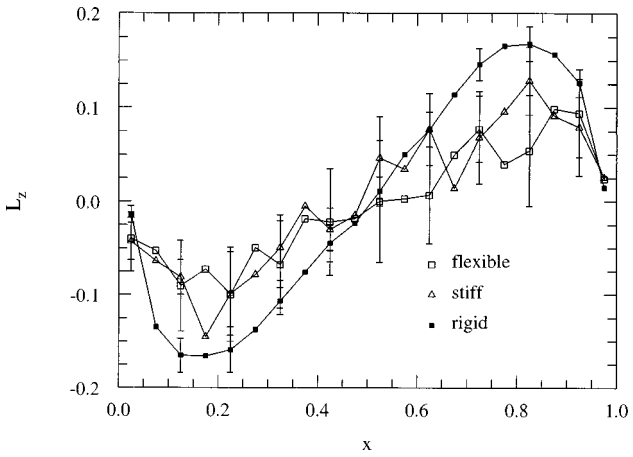

FIG. 2. Cross-stream angular-momentum profiles for the three types of molecule; the lines between the points are merely visual guides and some of the error bars have been omitted for clarity.

iting value, as has also been observed in studies of soft-sphere flow [13], and allowance has to be made for this aspect of the behavior in determining whether the limiting flow state had been attained.

It is to be expected that the three fluids will have different intrinsic properties, particularly the viscosity (see below). Meaningful comparison between flow properties of the different fluid models requires the simulations to be conducted under similar conditions, the most prominent of which is the maximum flow speed that occurs in the middle of the channel. A series of exploratory calculations provided estimates of the magnitude of g required to produce similar midstream flow speeds; the results described here used $g=0.025$, 0.035, and 0.05 (in reduced MD units) for the flexible, stiff, and rigid chains, respectively.

The measurements of the flow properties described below extend over a total interval of 250 time units (excluding the ''equilibration'' period). This overall time interval is subdivided into ten subintervals and the spread of the averages over the individual measurements is used to provide error bar estimates.

The most familiar feature of Poiseuille flow is the cross-stream velocity profile, which, for a Newtonian fluid, is parabolic in form. Figure 1 shows the measured profile (in reduced units) for the flexible, stiff, and rigid molecule fluids, based on a subdivision into 20 slices perpendicular to the x direction. The effectiveness of the nonslip boundaries is obvious; it is actually even better than is apparent from the figure, where each point represents an average over a slice whose thickness exceeds two monomer diameters. The curves represent the results of quadratic fits to the data, the motivation for which is the analytic solution for the Newtonian fluid. The fact that the profiles appear so close to parabolic is surprising in view of the complex x dependence of other aspects of the behavior, as described below; on the other hand, the fact that the parabolic profile also emerges from MD studies of monomer fluids flowing through channels whose width is a mere ten diameters [15] suggests that this kind of profile is particularly robust. Hard-sphere chains [2] were observed to produce similar results. From the fit to the theoretical velocity profile [3]

$$v_y(x)=\frac{\rho g D_x^2}{2\eta}\left[\frac{1}{4}-\left(x-\frac{1}{2}\right)^2\right], \tag{7}$$

where ρ is the density, η the shear viscosity, and D_x the channel width, the viscosity values follow immediately: $\eta=2.4$, 3.2 and 4.6 for the flexible, stiff, and rigid molecules, respectively. The trend is the expected one, with the viscosity increasing as reduced flexibility makes it harder for molecules to move relative to one another; rotation is an essential part of the shear motion and, because of its increased ability to deform, it is clearly easier for a short flexible chain to rotate in response to shear than a stiff one.

The cross-stream angular-momentum profiles for the three kinds of molecule are shown in Fig. 2; in this case the line segments joining the data points are included as visual guides only. The angular-momentum component measured is L_z; this is the only component with a nonzero average (since the x and y components should average to zero in the absence of any secondary flow pattern capable of breaking the underlying symmetry of the system). The magnitude of L_z reflects the local gradient of the velocity profile (the local shear rate); rotation is faster where shear rate is higher, except close to the channel walls where steric effects impede rotation. The rigid molecules have a larger maximum-angular-momentum value than the others and the stiff chains tend to have a slightly larger angular momentum than the flexible chains (intuitively, for chains with variable conformation, the angular momentum depends both on the overall spatial extent of the chain and on the rate at which it rotates about some axis, although there is no obvious way to isolate these contributory factors).

Though incidental to the main theme of this paper, it is interesting to compare the angular-momentum profile for the rigid molecules with a theoretical result valid at low Reynolds numbers. In terms of $x'=2x-1$, the z component of the angular velocity can be shown to have the form

$$\omega_z(x)=\frac{2v_m}{D_x}\left[x'-\frac{\sinh(\beta D_x x')}{\sinh(\beta D_x)}\right], \tag{8}$$

where $v_m=v_y(0.5)$ is the midstream flow speed and β a constant that depends on various properties of the fluid [9]. If

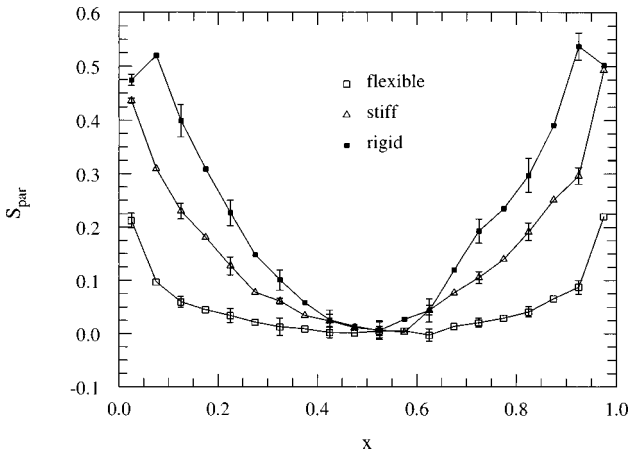

FIG. 3. Cross-stream values of the parallel order parameter.

we assume (falsely, as subsequent results show) that the molecules align in the xy plane, then $L_z = I\omega_z$, and if we define $l_0 = 2Iv_m/D_x$ and note that $I = 6.3$ for the molecules treated here, then $l_0 = 0.60$. The fit to the theoretical expression (not shown) is, with the exception of the one data point closest to each wall, essentially perfect; the fit yields $\beta D_x = 4.7$, but also produces $l_0 = 0.37$. However, given that the molecules are not required to lie in the xy plane, the effective value of I is reduced and this is likely to be the source of much of the discrepancy; a more detailed analysis of this behavior remains to be carried out. The corresponding result for dimers appears in [9].

In order to study orientational effects it is necessary to define order parameters suitable for providing quantitative estimates of the mean molecular alignment. For rigid molecules the solution is obvious, but for molecules with changing conformation there is no inherent unambiguous measure of orientational order. The technique used here follows the hard sphere studies [2], namely it focuses only on the imaginary line joining the monomers at the two ends of the chain and ignores other aspects of the internal arrangement. The orientation of chains that are in a relatively extended state is adequately described, even with this simplification, but if a chain is sufficiently contorted so that the ends approach one another (this is not the typical case for the short chains and relatively high shear rates employed here) the significance of such an order parameter is greatly diminished.

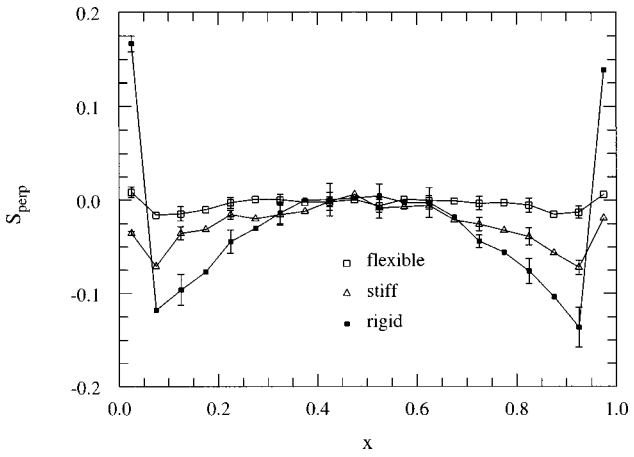

FIG. 4. Cross-stream values of the perpendicular order parameter.

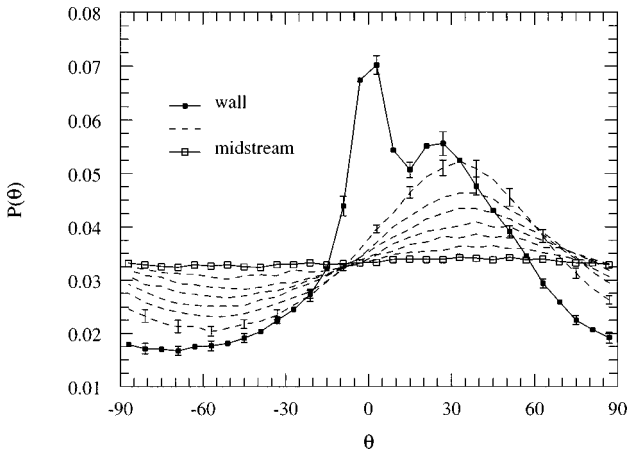

FIG. 5. Distribution of the chain orientation angle $P(\theta)$ for flexible molecules (the angle θ is defined in the text) measured over a series of slices parallel to the walls beginning at midstream and ending at the wall; typical error bars are shown.

The parallel order parameter provides an estimate of the degree of alignment in the plane normal to the channel walls that contains the parabolic velocity profile (i.e., the xy plane). We define

$$S_{\text{par}} = \left\langle \frac{\Delta y^2 - \Delta x^2}{\Delta x^2 + \Delta y^2 + \Delta z^2} \right\rangle; \tag{9}$$

Δx, etc., are the component magnitudes of the vector joining the terminal monomers in the case of chains with internal degrees of freedom or the molecular axis vector in the rigid case. $S_{\text{par}} = 1$ signifies complete alignment in the direction of flow. In order to establish whether there is any tendency to orient into, or away from, the xy plane, we also introduce a perpendicular order parameter

$$S_{\text{perp}} = \left\langle \frac{\Delta z^2}{\Delta x^2 + \Delta y^2 + \Delta z^2} - \frac{1}{3} \right\rangle. \tag{10}$$

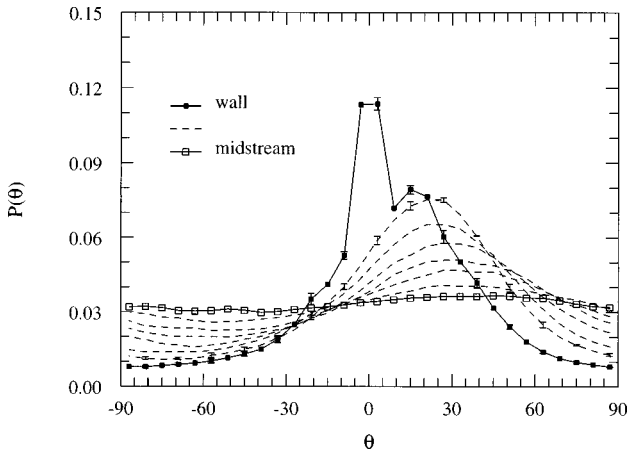

FIG. 6. Distribution of chain orientation angle for stiff molecules.

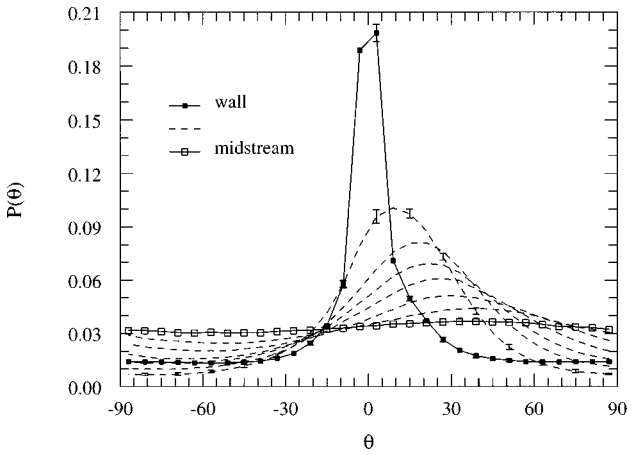

FIG. 7. Distribution of chain orientation angle for rigid molecules.

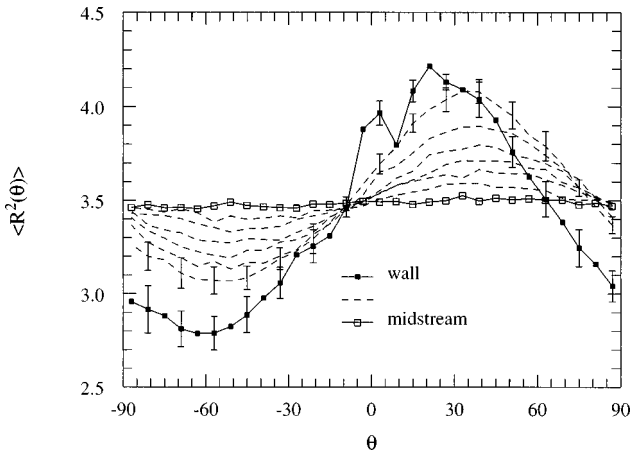

FIG. 8. Mean-square end-to-end distance distribution as a function of orientation angle for flexible molecules; $\langle R^2 \rangle$ is expressed in terms of the nominal bond length.

A value of $S_{\text{perp}} > 0$ indicates a certain tendency for the molecule to orient out of the xy plane, whereas a negative value corresponds to a preferred alignment within the plane.

Figures 3 and 4 show the cross-stream values of the two order parameters S_{par} and S_{perp}. Both are zero at midstream; there is no cause to align in this region since there is no shear. Away from the center there is an increasingly strong tendency for molecules to align both in the direction of flow and in the plane normal to the walls. Very close to the walls (in the first and last slices) the trend in behavior changes and for flexible and stiff chains the value of S_{perp} is seen to approach zero. The rigid molecules show much stronger wall proximity effects: S_{perp} is positive and comparatively large, which suggests that the preferred alignment very close to the walls is one that attempts to allow the rigid molecules to avoid the need to rotate at all; such behavior is consistent with the small drop in S_{par} near the walls.

A more detailed picture of molecular orientation can be obtained from the distribution of the orientation angle θ, defined as $\theta = \arctan(\Delta y/\Delta x)$, in each slice; once again, only terminal monomers are used to determine orientation in the case of nonrigid molecules. Due to mirror symmetry about the midstream yz plane, the results from the two halves of the system can be combined (after reversing the Δx values for one of the halves) and since the chain ends are equivalent, the actual range of θ (measured in degrees) is reduced to $\pm 90°$.

Figures 5–7 show the normalized orientation angle distributions for the three kinds of molecules, for a series of slices spanning the interval between the center of the channel and the wall. The flexible and stiff chains exhibit qualitatively similar behavior, although the peaks are stronger in the latter case (note that the vertical scales of the graphs differ); both kinds of chain show a pair of peaks in the curve corresponding to the slice closest to the wall. (The results are similar to those obtained for the hard-sphere chain models [2].) The peaks are even more pronounced for the rigid molecules, and in this case only a single strong peak is apparent for the slice adjacent to the wall. In this slice the peak occurs near $\theta = 0$, corresponding to a unimodal alignment distribution whose peak is in the direction of flow. The other peak occurs at an angle that increases as the molecules are located deeper within the bulk fluid. The preferred angle is clearly approaching, although perhaps never quite reaching, the Maxwell 45° value.

The molecular conformation itself also depends on proximity to the wall. Once again there is a certain degree of arbitrariness in quantifying this behavior so that, as before, the analysis will focus on the chain termini. One property of the chain that is expected to be particularly sensitive to the local shear rate is the mean-square end-to-end distance $\langle R^2 \rangle$; this quantity provides a measure of the degree to which chains exist in a contracted or extended state. Figures 8 and 9 show $\langle R^2 \rangle$ as a function of the orientation angle θ, for both flexible and stiff chains. Close to midstream there is no θ dependence, but as the wall is approached it is apparent that chains whose orientation to the flow is close to 45° are more stretched than average, while those perpendicular to this angle are more compact. In the slice closest to the wall, the stiff chains exhibit a significant peak in the flow direction and there is a weaker indication of similar behavior for the flexible chains as well.

A comparison of the flexible and stiff chains shows that the latter are more extended, as expected, but the range of variation of $\langle R^2 \rangle$ turns out to be much smaller for the stiff

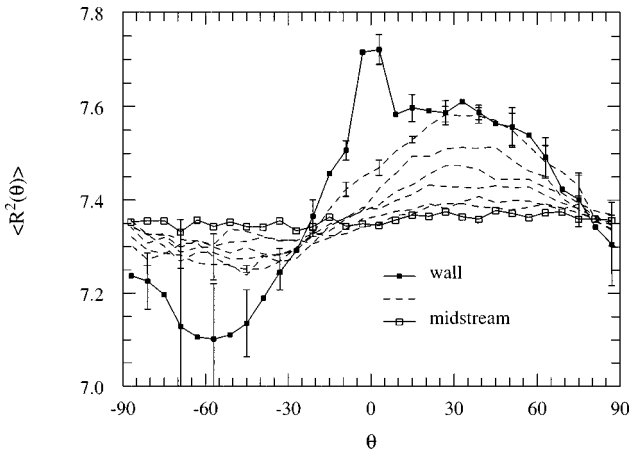

FIG. 9. Mean-square end-to-end distance distribution for stiff molecules.

chains; this is a consequence of the next-nearest-neighbor bonds that restrict the allowed conformations (there are only two such bonds in a chain of four monomers, so that their effect is more pronounced than it would be in longer chains). For flexible chains $\langle R^2 \rangle = 3.5 \times (\text{bond length})^2$ at midstream (where there are essentially no shear effects); for completely random three-step walks the value of the prefactor is 3 [16] and the reason that the prefactor is larger than this is primarily due to the excluded-volume effect. The stiff chain prefactor 7.4 is greater still, as a consequence of the next-nearest-neighbor bonds, but this lies below the value of 9 for a fully rigid molecule consisting of four monomers.

IV. CONCLUSION

In this paper we have described MD simulations of the shear flow of short linear molecules in a channel bounded by two parallel, rough walls. In order to examine the effect on the flow of chain flexibility, completely flexible and partially stiffened chains have been considered and by way of contrast the limiting case of completely rigid molecules of similar length has also been studied.

The results clearly reveal the complex behavior that is present in even this very limited model of an oligomer fluid. Strong rotational and orientational effects are seen to occur throughout the flow. Near the walls, competition appears between two opposing trends: on the one hand, the desire to rotate to reduce the shear resistance and also to attain maximum elongation when aligned at 45° to the flow, but, on the other hand, a tendency to orient parallel to the wall, with a hint (for rigid molecules) of some alignment normal to the flow direction to reduce the need for the molecules to rotate. One surprising outcome is that, despite these complex trends, the overall velocity profile remains parabolic, exactly as observed both in the flow of simple monatomic fluids and in the analytic solution of the continuum equations for a Newtonian fluid; in some sense the parabolic profile is sufficiently robust not to be affected by issues of molecular rotation and orientation.

[1] R. B. Bird and C. F. Curtis, Phys. Today **37 (1)**, 36 (1984).
[2] D. C. Rapaport, Europhys. Lett. **26**, 401 (1994).
[3] L. D. Landau and E. M. Lifshitz, *Fluid Mechanics* (Pergamon, Oxford, 1959).
[4] J. C. Maxwell, Proc. R. Soc. London, Ser. A **22**, 46 (1873).
[5] T. A. Weber and N. D. Annan, Mol. Phys. **46**, 193 (1982).
[6] D. Brown and J. H. R. Clarke, Chem. Phys. Lett. **98**, 579 (1983).
[7] R. Edberg, G. P. Morriss, and D. J. Evans, J. Chem. Phys. **86**, 4555 (1987); R. Edberg, D. J. Evans, and G. P. Morriss, Mol. Phys. **62**, 1357 (1987).
[8] T. Weider, U. Stottut, W. Loose, and S. Hess, Physica A **174**, 1 (1991).
[9] K. P. Travis, B. D. Todd, and D. J. Evans, Physica A **240**, 315 (1997).
[10] Z.-R. Chen *et al.*, Science **277**, 1248 (1997).
[11] D. C. Rapaport, Comput. Phys. Rep. **9**, 1 (1988).
[12] W. Smith and D. C. Rapaport, Mol. Simul. **9**, 25 (1992).
[13] D. C. Rapaport, *The Art of Molecular Dynamics Simulation* (Cambridge University Press, Cambridge, 1995).
[14] W. T. Ashurst and W. G. Hoover, Phys. Rev. A **11**, 658 (1975).
[15] K. P. Travis, B. D. Todd, and D. J. Evans, Phys. Rev. E **55**, 4288 (1997).
[16] P. J. Flory, *Statistical Mechanics of Chain Molecules* (Wiley, New York, 1969).